Magnetoresistance of the spin-state-transition compound $La_{1-x}Sr_xCoO_3$

R. Mahendiran and A. K. Raychaudhuri
Department of Physics, Indian Institute of Science, Bangalore–560 012, India
(Received 1 April 1996)

We have investigated the magnetoresistance (MR) of the perovskite oxide $La_{1-x}Sr_xCoO_3$ for $0 \leqslant x \leqslant 0.4$ which shows a spin-state transition from low-spin Co^{III} to high-spin Co^{3+} as a function of temperature. In the metallic compositions ($x \geqslant 0.25$) appreciable MR occurs only near the ferromagnetic Curie temperature. For the most metallic composition $x=0.4$, there is a small positive contribution to the MR near the T_c. In the insulating samples ($x \leqslant 0.2$) the MR shows a large hysteresis which depends on the temperature. The value of the MR is negative and large in the insulating compositions and shows a maximum near the temperature where magnetic studies showed a spin-glass-like transition. We also find a strong role of the spin-state transition of the Co^{3+} ions in the electronic transport leading to a characteristic behavior of the MR in the Co^{3+}-rich insulating samples. [S0163-1829(96)01645-1]

I. INTRODUCTION

The recent discovery of giant magnetoresistance (GMR) in Mn-based oxides[1–11] $L_{1-x}A_xMnO_3$ (L=La, Nd, Pr, etc., and A=Ca, Sr, Ba, Pb, etc.) has led to further investigation of the physical and chemical properties of these oxides in detail. Unlike Mn-based oxides (manganates), there are very few reports on the magnetoresistance behavior of Co-based oxides (cobaltates).[12–14] Even though hole doping (by substitution of Sr^{2+} for La^{3+}) in antiferromagnetic (AFM) insulating $LaMnO_3$ as well as in $LaCoO_3$ renders ferromagnetism (FM) and metallicity, there are certain differences between these two systems in spin structure. We elaborate these differences below. The present MR results indicate that these differences between the two systems should be taken into account to ascertain whether MR arises from the same origin.

Sr substitution in $LaMnO_3$ leads to the conversion of Mn^{3+} ($t_{2g}^3e_g^1$, $S=2$) into Mn^{4+} (t_{2g}^3, $S=3/2$). Magnetic studies on this system show that there is a core spin arising from 1/2-filled t_{2g}^3 levels. Since the exchange energy is larger than the crystal field energy, the high-spin state is stable in Mn-based systems. No thermal variation of the spin state of the Mn ion has been reported so far. A strong Hund's rule coupling of the core spin with the more mobile carriers (hole or electron) in the e_g orbitals determines most of the observable behavior of the Mn-based system. However, in $LaCoO_3$, the Co ion is predominantly in low-spin-state Co^{III} (t_{2g}^6, $S=0$) at low temperature, and with increases in temperature, a progressive conversion of low-spin Co^{III} into high-spin Co^{3+} ($t_{2g}^4e_g^2$, $S=2$) takes place.[15–18] This happens because at low temperature a large crystal field stabilizes the low-spin state. However, the energy difference between the two spin states being low (≈ 0.03 eV), thermal excitation can provide a transition to a high-spin configuration. In the temperature range 100 K $\leqslant T \leqslant$ 350 K, the ratio of high-spin to low-spin Co reaches 50 : 50 with short-range ordering of low-spin and high-spin Co ions[18] and above 600 K $LaCoO_3$ shows metallic behavior.[16,17] On Sr substitution, tetravalent Co ions are created. They can be low-spin Co^{IV} (t_{2g}^5, $S=1/2$) or high-spin Co^{4+} ($t_{2g}^3e_g^2$, $S=5/2$). Recent electron spectroscopy[24] results show that high-spin Co^{4+} is ≈ 1 eV lower in energy than low-spin Co^{IV}. Sr-substituted $La_{1-x}Sr_xCoO_3$ thus contains a mixture of low-spin Co^{III} (t_{2g}^6), low-spin Co^{IV}(t_{2g}^5), and some high-spin Co^{3+} ($t_{2g}^4e_g^2$) and high-spin Co^{4+}($t_{2g}^3e_g^2$) depending on the temperature as well as the value of x.

The absence of a half-filled t_{2g} orbital in the low-spin Co ion gives rise to less strong Hund's rule coupling of the carrier to the core spin. This is an important fact that distinguishes the Co system from the Mn system. We show in this paper that these aspects of the Co ions along with the spin-state transition of the Co^{3+} ions are essential ingredients in understanding the MR data.

The superexchange interaction Co^{IV}-O-Co^{3+} or Co^{4+}-O-Co^{3+} is known to be ferromagnetic and the exchange intereactions between the ions with the same valency state are antiferromagnetic.[15–18] Whether the ferromagnetism in cobaltates is mediated by a double-exchange mechanism or not is clearly not understood at present. However, the absence of the half-filled t_{2g} level providing the core spin and a strong Hund's rule coupling, unlike the manganates, make this mechanism a less likely possibility.

At this stage it will be worthwhile to consider the magnetic phase diagram of $La_{1-x}Sr_xCoO_3$ as has been proposed by different investigators[18–21] as shown in Fig. 1. As we will see below the magnetic phase diagram helps us to understand MR data as well as the zero-field resistivity data to be reported in this paper. It can be seen that there are two distinct regions in the phase diagram. For $x>0.2$–0.25 one sees the onset of ferromagnetic transition (denoted by T_c) but the resulting ferromagnetic state does not have a long-range order. Rather it becomes like a cluster of ferromagnetic regions embedded in a nonferromagnetic matrix. For $x<0.1$, one observes a spin-glass-like state at lower temperature and there seems to exist a spin-state-transition temperature marked by T_s in this region. In the transition region $0.2>x>0.1$ the behavior seems to be more complicated and there seems to be disagreement between different investigators. We avoided this region (shaded in Fig. 1) in the present work. The data

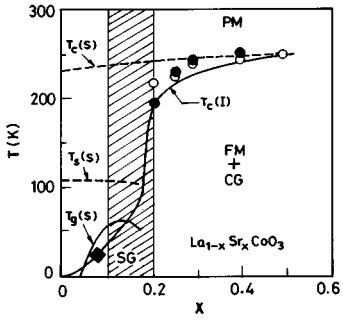

FIG. 1. The schematic phase diagram of $La_{1-x}Sr_xCoO_3$. The Sr concentration (x) is shown along the X axis. The $T_c(S)$ and $T_c(I)$ represent the profile of the ferromagnetic transition temperature from Refs. 18 and 19, respectively. The open and solid circles correspond to that of the T_c value reported in Ref. 20 and the present investigation, respectively. The solid square represents the value taken from Ref. 21. $T_s(S)$ is the spin-state-transition temperature from Ref. 18. SG, spin glass; CG, cluster glass; FM, ferromagnetic metal; PM, paramagnetic metal. The hatched region is the transition region.

presented here include the region $x \leqslant 0.1$ and $x \geqslant 0.2$. The main objective of this paper is to study MR for samples with different x and correlate our observation with the magnetic phase diagram. In particular, for $x \leqslant 0.1$ (in the region of the onset of spin-glass behavior) no MR data has been reported so far. We have carried out measurements of resistivity (ρ), magnetoresistance (MR$=[\rho(H)-\rho(0)]/\rho(0)$, where $\rho(0)$ and ρ(H) are the resistivities at zero field and at a field of H Tesla, respectively), and ac χ on the samples for $0 \leqslant x \leqslant 0.4$.

II. EXPERIMENTAL DETAILS

The compounds of $La_{1-x}Sr_xCoO_3$ ($0 \leqslant x \leqslant 0.4$) were prepared by the ceramic method staring with predried La_2O_3, $CoC_2O_4 \cdot 2H_2O$, and $SrCO_3$. Accurately weighed amounts of the reactants in required proportions were mixed and ground together with acetone. The mixture was heated at 1100 °C for 1 day. The mixture was then ground again, pelletized, and heated at 1100 °C in air for 3 days. The phase purity was checked with x rays and the samples were found to be of single phase and the diffraction pattern compared well with the reported data.

The resistivity was measured by the four-probe method using an ac bridge operating at 20 Hz. The magnetoresistance measurement was done with a superconducting solenoid immersed in liquid He. The ac susceptiblity (at 2 mT and 77 K $\leqslant T \leqslant$ 400 K) was measured by mutual inductance bridge operating at 100 Hz.

III. RESULTS AND DISCUSSION

A. ac susceptibility

The ac susceptibility (χ) of the sample with $x \geqslant 0.1$ is shown in Fig. 2 (for the samples with less Sr content our bridge was not sensitive enough to locate any transition). The T_c's of the samples are 190 K, 240 K, 240 K, and 245 K for $x=0.2$, 0.25, 0.3, and 0.4 compositions, respectively. For

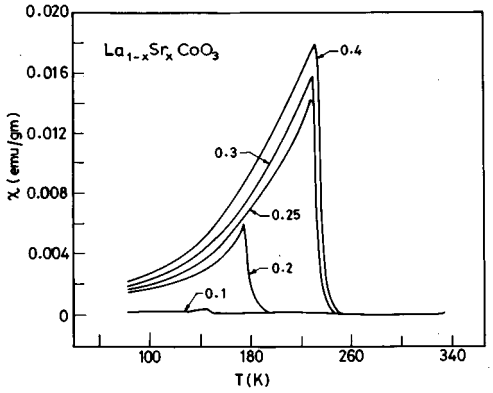

FIG. 2. The magnetic susceptibity (ac χ) for $La_{1-x}Sr_xCoO_3$.

$x=0.1$ composition susceptibility rises noticeably below 150 K but the value of χ is very small compared to the other samples. This rise in χ may mean the formation of local ferromagnetic clusters or regions in which spins have ferromagnetic correlation over considerable length scales. The T_c's of our samples are very close to those found in previous studies.[18–20] We see that the onset of the FM transition is rather sharp at least for samples with $x \geqslant 0.2$. The ac χ's of all the samples (measured at 2 mT) show a peak at a temperature close to but lower than T_c and then come down rather prominently as the temperature is lowered. The temperature dependence of χ below T_c is very similar to the field-cooled (FC) dc magnetization measured at 2 mT by Itoh *et al.*[19] and similar to that of Ganguly *et al.*[20] It is this particular behavior along with the time dependence of the magnetization (M) seen in Ref. 19 as well as the lack of proper saturation of (M) even in fields as high as 5–6 T that points to the fact that the ferromagnetic order seen in the cobaltates lacks proper long-range order. (This is in sharp contrast to manganates[7] where all the properties of a long-range ferromagnet are seen for $x=0.3$.)

The rapid fall of χ in the ferromagnetic state can come from essentially two sources. The initial susceptibility $\chi(T) \propto M_s(T)^2/K(T)$, where $M_s(T)$ is the saturation magnetization at the temperature T and $K(T)$ is the anisotropy energy density. $\chi(T)$ will decrease if $K(T)$ increase or $M_s(T)$ decrease. The previous[22] magnetization data for samples with $x>0.2$ show that the M_s measured at a higher field has the normal temperature dependence of the M_s as expected of a ferromagnet and does not decrease at low temperature. One would therefore conclude that the decrease of χ below T_c arises because of an increase of the anisotropic energy density on cooling below T_c. This anisotropic energy blocks the spins and forbids them to respond to a weaker magnetic field. As we see below, the signature of this strong anisotropy is shown up as a marked hysteresis of MR on field cycling for the insulating samples ($x \leqslant 0.1$). Our results on the ac susceptibility therefore serve as a magnetic characterization of the samples used in the subsequent transport measurement studies as well as are a reconfirmation of some of the previous observations.

IV. RESISTIVITY IN ZERO FIELD

A. Insulating samples

The zero-field resistivity (ρ) of the samples is shown in Fig. 3. The resistivity decreases with increasing x and the

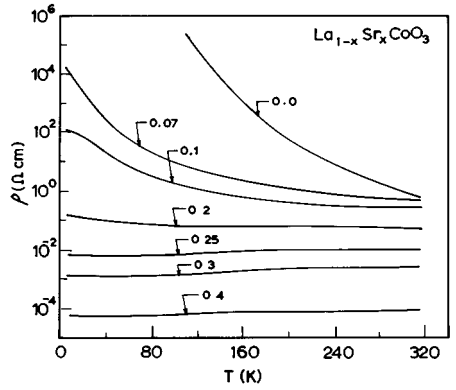

FIG. 3. The temperature dependence of the resistivity (ρ) of $La_{1-x}Sr_xCoO_3$.

behavior of the temperature dependence of ρ changes abruptly around the composition $x=0.2$ (see Fig. 6 for clarity). For the $x=0$ sample the resistivity becomes too high below 100 K to be measurable by our apparatus and also for this sample the contact resistance become very high so that even a four-probe measurement starts to give error. We found that the $\rho(T)$ for these samples follows the behavior

$$\rho(T)=\rho_0\exp[(T_0/T)^n], \tag{1}$$

where $n=\frac{1}{2}$. This is the signature of variable range hopping (VRH) in the presence of a Coulomb gap in the density of states or Efros-Shlovskii- (ES-) type hopping.[23] (To distinguish it from the regular VRH hopping where $n=\frac{1}{2}$ we call this ES hopping.) We demonstrate this in Fig. 4 where we have plotted $\ln\rho(T)$ vs $T^{-1/2}$. For the $x=0$ sample the temperature region of data is very limited. Though in the limited range the data fit to Eq. (1) we find that the fit does not give physically rational parameters. This is because the values of T_0 ($=2\times10^5$ K) and ρ_0 ($=4.6\times10^{-10}$ Ω cm) are physically unjustifiable. So for this sample we think that the fit to Eq. (1) is just an accident. For this it may be good to talk about an Arrhenius-type relation [$n=1$ in Eq. (1)] with an activation gap $=0.2$ eV. For the other insulating samples the ES type of hopping for $T<130$ K seems to be a physical possibility. The values of T_0 are 3965 K, 1902 K, and 37 K

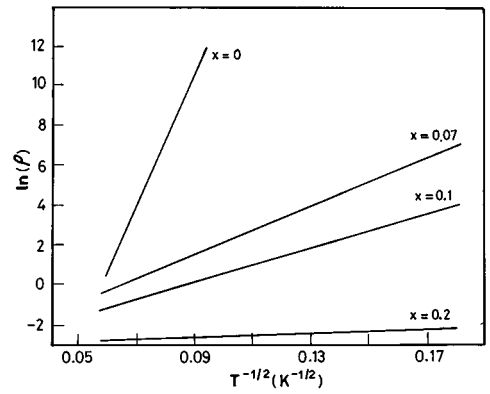

FIG. 4. The Efros-Slovskii type of conduction in the insulating samples.

and ρ_0 are 20.5 mΩ cm, 23.6 mΩ cm, and 45.7 mΩ cm for $x=0.07$, 0.1, and 0.2 samples, respectively. This is the correct order of ρ_0. (Note that ρ_0 is generally of the order of $1/\sigma_{\rm Mott}$, where $\sigma_{\rm Mott}$ is the Mott minimum conductiviity in these samples.) For most materials ρ starts to show a negative $d\rho/dT$ when $\rho<1/\sigma_{\rm Mott}$. It can be seen from our data of the $x=0.2$ sample (see Fig. 6) that the activated behavior starts when the resistivity becomes higher than 50 mΩ cm. So we conclude that the values of ρ_0 obtained from the fit are physically justifiable. The values of T_0 for the samples with $x=0.07$ and 0.1 are also reasonable; however, for the sample $x=0.2$ the value of T_0 is too low and this is expected because the sample is close to the *M-I* transition boundary. In fact Eq. (1) is valid only for the region $T\ll T_0$. As a result, relation (1) for this sample should really be tested much below 4 K and we therefore do not assign much significance to the value of T_0 for this sample except for noting that it is close to the *M-I* transition boundary. For the samples $x=0.07$ and $x=0.1$ we tried to estimate a localization length $\langle\xi\rangle$ from the values of T_0 using the relation[23]

$$k_BT_0=1.5e^2/(\kappa\langle\xi\rangle), \tag{2}$$

where e is the electronic charge and κ is the dielectric constant. The numerical factor (1.5) is an esitmate and depends somewhat on how far one is from the critical *M-I* transition point. Using Eq. (2) we find that for the $x=0.07$ sample the localization length $\langle\xi\rangle\approx7.1$ Å and for the $x=0.1$ sample this is ≈15 Å. (For these estimates we used $\kappa=10$. The exact value of the $\langle\xi\rangle$ will depend on the proper knowledge of κ.) These values are of the order of a few (2–4) lattice spacings. For these samples the value of the pseudocubic lattice parameter $\mathbf{a}_c$ is around 3.83 Å. This is the approximate length of a Co-O-Co bond. This implies that the charge can travel a distance of a few lattice spacings even when the substitution level is only $x=0.1$. As x approaches the critical composition $x=0.2$ from below, the value of $\langle\xi\rangle$ becomes larger and eventually it will diverge at the critical composition. For the samples with $x\leqslant0.2$ the charge carriers are predominantly hole type. This can be concluded from the thermopower data.[18,26] If we assign one hole carrier to each Co^{4+} ions created by substitution by one Sr^{2+}, we find that the mean distance between the donors ($\langle r_s\rangle$) is around $1.5\mathbf{a}_c$ for the $x=0.07$ sample and $1.34\mathbf{a}_c$ for the $x=0.1$ sample. For the $x=0.2$ sample this becomes $0.98\mathbf{a}_c$ and we have the *M-I* transition. The ratio $\langle\xi\rangle/\langle r_s\rangle$ is already >1 for the samples with $x=0.07$ and they will increase as x approaches 0.2. We carried out the above discussions to set the length scale of the electronic conduction in these materials. This is an important parameter in the analysis of our MR data. Because if the carriers are confined only to one unit cell (or over a distance of one Co-O-Co bond) and there is a ferromagnetic correlation of spins over a few lattice spacings, then the carriers will not be affected by the cluster nature of the magnetic spins. The cluster nature of the spin order will affect the MR significantly if the spin correlation length is comparable to the localization length.

B. Metallic samples

For the samples with $x\geqslant0.25$ the behavior of ρ for most of the temperature range is metallic and the value of ρ de-

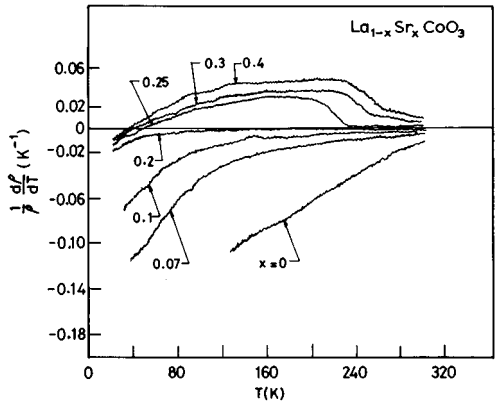

FIG. 5. The scaled temperature derivative $[(1/\rho)(d\rho/dT)]$ of $La_{1-x}Sr_xCoO_3$ as a function of temperature. Note the increase in the value of the derivative near T_c in the metallic samples.

creases drastically as the Sr content (i.e., x) is increased. In order to see the manifestations of the magnetic transition associated with the samples, we show in Fig. 5 the scaled temperature derivative $(1/\rho)(d\rho/dT)$ as a function of temperature. One can clearly see that there is a change in slope at $T=T_c$ in all the samples. We can assign the change in slope as a gradual decrease of the spin-disorder scattering (as in a conventional ferromagnet) on the onset of FM order. It is also interesting that the scaled slope in all the samples increases as the samples become more metallic. In fact, for the $x=0.25$ sample it is almost zero for $T>T_c$ and it is slightly negative for the sample with $x=0.2$. The sample with $x=0.2$ needs special mention as it is at the boundary of the M-I transition. This composition is close to but larger than the composition $x=0.18$ where one sees the onset of FM order. Though the value of ρ for this material is much smaller than those of the samples with smaller x, it shows an insulatorlike behavior at $T<100$ K as mentioned in the above subsection. Above 100 K, ρ shows a rather shallow temperature dependence with a broad hump at around 190–200 K which is very close to the T_c of this material (see Fig. 6). We can assign the broad hump in the ρ at $T=190-200$ K to the FM transition and to the decrease of the spin disorder scattering on the onset of FM order. Though the $(d\rho/dT)$ is <0 in this composition for $T>T_c$, we think that at higher temperature it has itinerant carriers albeit like a marginal metal[25] and a perceptible contribution to ρ arises from the spin-disorder scattering which gets frozen out as T is decreased below T_c, giving rise to the broad hump.

The rapid rise in ρ for $T<100$ K may be related to the onset of the spin-state transition of trivalent Co ions from a high-spin to low-spin state. In fact we have the signature of this transition even in the metallic samples. It can be seen that below 50 K in all the samples we have a small rise in ρ as the temperature is decreased (see Figs. 5 and 6). In Fig. 5 this shows up as a negative $(d\rho/dT)$ at the lowest temperatures. Such a small rise in ρ at low temperatures has been seen in a number of metallic oxides[25] and this does not necessarily mean entry into a nonmetallic phase. This small rise can arise from disorder-induced effects. However, since in all the samples (irrespective of their ρ) the onset of the low-temperature rise occurs at around the same temperature, other causes like the spin-state transition of the trivalent Co ions can also be a possibility. We suggest the following scenario for the electronic transport which agrees well with the magnetic phase diagram for the samples (see Fig. 1).

The FM as well as the metallic behavior in these samples is related to the formation of Co^{4+} (or Co^{IV}) ions on Sr^{2+} substitution. The magnetic data[18,19] suggest a lack of proper long-range ferromagnetic order and a cluster-glass-type behavior. Therfore this material seems to contain ferromagnetic clusters (containing Co^{4+} or Co^{IV}) which are metallic and an intercluster medium which is semiconducting and contains trivalent Co ions both in the high-spin and low-spin states whose population depends on the temperature. [It has been shown[18] from magnetic studies on samples with low Sr substitution that for 135 K $<T<300$ K the populations for the two spin states are around 50% each and for $T<100$ K most of the trivalent Co ions go to the low-spin $(S=0)$ state.] For $x\geq 0.2$, the ferromagnetic clusters containing predominantly Co^{4+} percolate to form a large macrosopic cluster which shows up as a bulk ferromagnetic transition. However, the connecting regions of these clusters contain trivalent Co ions which act like a temperature-dependent ''switch'' between the clusters. It permits charge transport when the Co ion is in a high-spin state (Co^{3+}) and localizes carriers in the cluster when in the low-spin state (Co^{III}). (In polycrystalline materials these trivalent Co ions can reside also in crystallographic grain boundaries.) The effect of this can be particularly seen for the sample with $x=0.2$ which is very close to the percolation threshold. Its electrical conductivity will have comparable contributions coming from the FM clusters as well as from the intercluster medium. As the temperaure goes below 100 K the spin-state transition will make the most of the Co^{3+} ions to go to the low-spin state and thus gradually localizing the carriers in the FM clusters. Then, this will show up as a large rise in ρ for $T<100$ K. For materials with $x\geq 0.25$ which have a concentration of metallic and FM clusters well beyond the percolation threshold, the conduction is mostly metallic with a small contribution coming from the trivalent Co ions residing at the surface of the clusters. As a result the effect of the spin-state transition is very much suppressed. Nevertheless, it makes a distinct mark on ρ at low temperatures. Thus the resistivity behavior has a clear signature of the spin-state transition of the trivalent Co ions. (Note that we exercise caution over here. It has not yet been settled beyond doubt[18,21] if the high-spin–low-spin transition of the Co ions seen in the pure $LaCoO_3$ persists even when Sr is doped into the system. Our resistivity data add evidence for the existence of the spin-state transition at least in the presence of dilute Sr substitution.) Below, we present and analyze the magnetoresistance data in view of the above physical picture.

V. MAGNETORESISTANCE

The magnetoresistance of the samples shows rather fascinating behavior and depends very crucially on the level of Sr substitution. For the metallic and ferromagnetic sides the MR is mostly negative and it is typical of a ferromagnetic metal. But for $x<0.2$ the MR becomes large (and negative). In fact there is a qualitative difference of the nature of MR for the

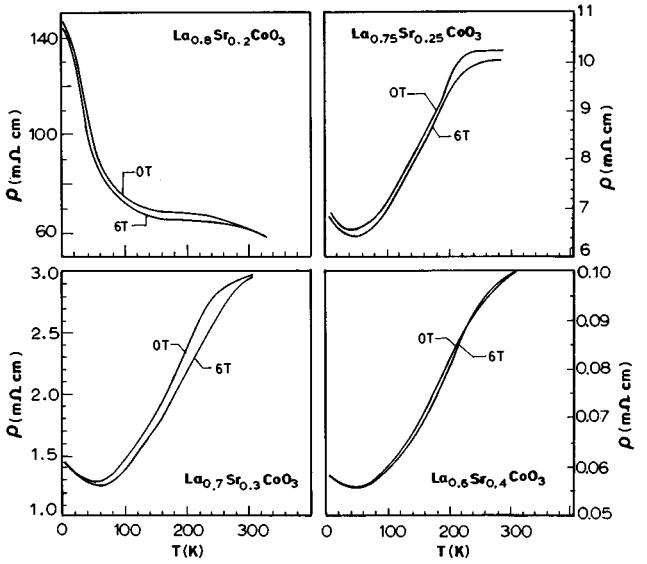

FIG. 6. The temperature dependence of resistivity in zero field (0 T) and in the field of 6 Tesla (6 T) for the compositions $x=0.2$, 0.25, 0.3, and 0.4.

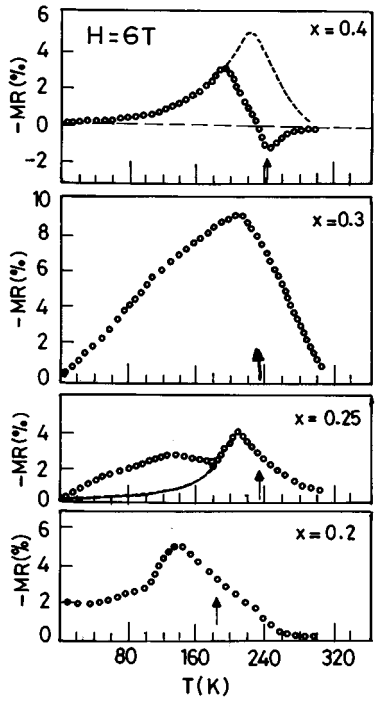

FIG. 7. Magnetoresistance (MR) as a function of temperature for $x=0.2$, 0.25, 0.3, and 0.4. (Note that MR is plotted along the positive Y axis.)

samples with $x \geqslant 0.2$ and $x < 0.2$. In this paper we would like to bring this particular aspect into focus. We first show the MR data of the more metallic samples. Preliminary MR data at $T=4.2$ K for the metallic samples have been reported by us earlier.[12] The MR in these materials is found to be isotropic as in manganates. The samples in the present studies are different from those used in the preliminary report and we present here the data of all the samples for the complete temperature range $T \leqslant 300$ K.

A. Magnetoresistance (MR) of the metallic samples ($x \geqslant 0.2$)

The MR data for the more metallic samples are shown in Figs. 6 and 7. In Fig. 6 we show the ρ as a function of temperature in zero field as well as in a field of 6 T. In Fig. 7 we show the MR as a function of temperature in a field of 6 T. We have shown the negative MR along the positive Y axis. For $T<T_c$ the MR is negative for all the samples. It can be seen that as the sample becomes more metallic the MR decreases and in the most metallic sample ($x=0.4$) it has a positive contribution which shows up when the negative contribution becomes small at $T \approx T_c$ or at $T>T_c$. If this positive contribution would not have been there, the $x=0.4$ sample would have shown a peak close to T_c (marked by a downward arrow in the graph) as in the $x=0.3$ and $x=0.25$ samples. The expected behavior in the absence of the positive contribution is sketched as a dashed line in Fig. 7. In fact the positive contribution for the $x=0.4$ sample deserves attention. Such a positive contribution has also been seen in a closely related ferromagnetic metallic oxide $SrRuO_3$ (Ref. 27). The origin for this positive MR in ferromagnetic metallic oxides has not yet been explained. This is a small effect compared to very large negative MR seen in the oxides in general and therefore it often escapes attention. There are two aspects to this positive MR. First, it can come from the conventional orbital effects as in any other metal but its magnitude is distinctly orders of magnitude higher than what one expects to see in a conductor of such resistivities at such a high temperature. Second, we find that the positive MR may have a link to the FM transition as well because it shows an enhancement near T_c. A detailed investigation of this positive MR in metallic ferromagnetic oxides will definitely be worthwhile.

For the $x=0.3$ and $x=0.25$ samples, the highest value of MR is seen close to T_c. The value of the MR even at the peak is much smaller than that of the manganates. This behavior of the metallic samples, showing a peak in the negative MR close to T_c, is a normal behavior expected of a metallic ferromagnet (like Ni) whose spin-disorder scattering is suppressed on application of the magnetic field, the scattering being strongest near the T_c and the negative MR also the largest. For the sample $x=0.25$ which is barely on the metallic side, an additional contribution starts to show up. This additional contribution is negative and small but distinctly present. This contribution shows a broad peak around 130–140 K. This new contribution to the MR becomes clearer for the $x=0.2$ sample. In this sample the MR does not show a peak at T_c. This is expected because the contribution of the spin-disorder scattering to the resistivity is small in this sample. As a result the conventional negative MR seen near T_c in a ferromagnetic metal is not seen in this material. The new contribution, as explained in the next subsection, has its origin linked to the random freezing of ferromagnetic clusters (or a spin-glass-like transition) which have been seen for the samples with less x. For this material ($x=0.2$) there will be larger clusters which link up to show a ferromagnetic transition. But there will be a substantial number of smaller clusters which will freeze in random directions. The field dependence of MR in the metallic sample

at a given temperature is almost linear as reported before.[12,14] The magnitude as well as the field dependence of the MR in the cobaltates is much different from those in the manganates. The difference in spin structure and the nature of the ferromagnetism and MR behavior in cobaltates point to the fact that a Zener double-exchange mechanism may be less operative here, unlike in the manganates.

The annealing condition changes the value of resistivity and MR but not the main qualitative feautures of MR. The previously reported[12] samples were annealed at 1000 °C for 24 h and had distinctly higher resistivities than the present samples which were annealed at 1100 °C for much longer duration. The annealing condition by changing the oxygen stoichiometry changes the Co^{4+}/Co^{3+} ratio, leading to changes in the physical properties. In this paper we made all the samples with the same preparative condition so that the internal consistency is preserved and the systematics are not affected.

B. Magnetoresistance of the insulating samples

We have just seen that as the sample approaches the insulating side the ferromagnetism is suppressed and along with that the negative peak of the MR, characteristic of a metallic ferromagnet, seen near the T_c is also suppressed. Instead, a new negative contribution to the MR showing up at lower temperatures starts taking over. The more insulating samples which have no ferromagnetic order show this new contribution as a rather giant effect.

In Fig. 8, we show the data for the three insulating samples. Here we plot the fractional resistivity change as a function of the magnetic field at a given temperature. In these materials we could not do the measurements in the way we have done for the metallic samples (i.e., fix the field and vary the temperature) because of the strong hysteresis and dependence of the data on the magnetic history. Under such conditions, a number of ''memory'' effects are seen which unfortunately make the observation very complicated. To stick to the basic observation of the MR we followed the route mentioned below. The samples were first cooled in zero field to the lowest temperature and then the applied magnetic field was increased from 0 T to 6 T and gradually decreased back to 0 T . The field ramp up and down rates are 0.01 T/sec. The samples were then warmed up to above 300 K and then cooled down again in zero field to the new temperature and the field data were taken. If the warming up to above room temperature (before any new temperature point) is not done, then the data are completely history dependent and often conflicting. It is important that the sample be prepared fresh (without any field history) before application of the field at every temperature. This, however, makes the experiment very time consuming. We see that as the field is increased the resistivity decreases almost linearly and shows no sign of saturation up to a field of 6 T. When the field is decreased, ρ does not increase again but in all the three samples ρ actually decreases somewhat when the field is decreased to zero. (This happens mostly at higher temperatures $T>100$ K.) This leads to a nonclosure of the resistivity at the zero field. For the $x=0$ sample for which we could do the measurements down to 130 K this behavior persists until the lowest temperature. But for the less resistive $x=0.07$ and

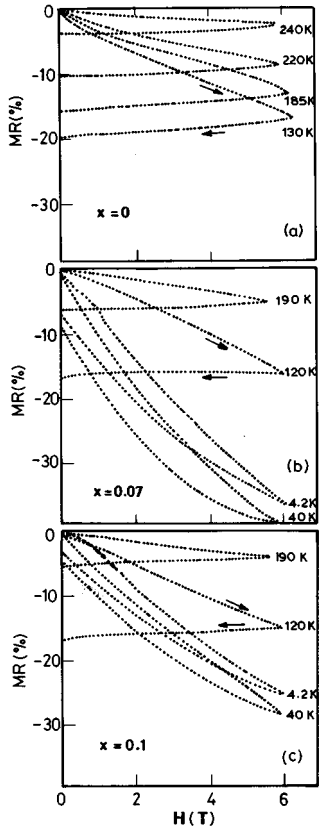

FIG. 8. The MR of insulating compositions $x=0$, 0.07, and 0.1 as a function of the applied field. The arrow indicates the direction of field sweep.

$x=0.1$ samples the very strong hysteresis and the resistivity nonclosure actually become very small at lower temperatures although the actual value of the MR is higher at lower temperatures (see data at 4.2 K and 40 K). We have demonstrated this in Fig. 9 where we have plotted the MR at field 6 T as a function of temperature and in the inset we showed the resistivity nonclosure (α). The data have been taken from

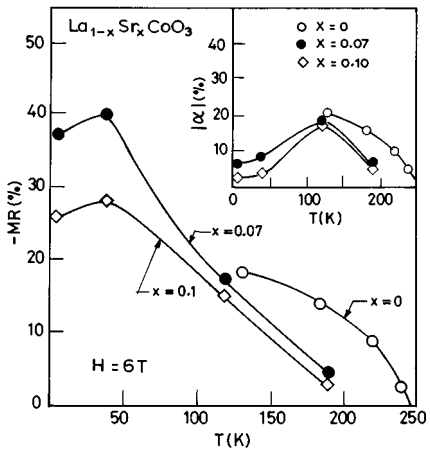

FIG. 9. The MR (at 6 T) as a function of T for the insulating samples. The inset shows the extent of hysteresis nonclosure of the MR after a field cycle (see text for details).

Fig. 8. We define the resistivity nonclosure as $\alpha=[\rho_0^+-\rho_0^-]/\rho_0^+$ where ρ_0^+ is the resistivity of a virgin sample (before application of a field) and ρ_0^- is the resistivity of the same sample when the field is brought back to zero again after ramping up to 6 T. Both MR and α in all the samples are very small above 250 K. This is the temperature of the bulk ferromagnetic transition and also the temperature of the formation of ferromagnetically correlated regions in the Sr-substituted systems. It is therefore clear that the magnetic field will have a perceptible effect (leading to a negative MR) only when the temperature is low enough compared to the energy involved in the ferromagnetic exchange so that cluster formation can take place, leading to a significant contribution to the MR. As the temperature is decreased below 250 K, the MR as well as the α rises rapidly. For the $x=0.07$ and 0.1 samples the MR continues to rise at lower temperatures, eventually showing a maximum in the temperature range around 40–50 K which is close to the spin-glass-like transition temperature (T_g) seen in the two materials (see Fig. 1). Interestingly, α shows a maximum at much higher temperature ($T=120$–140 K). Due to the paucity in the data points, these temperatures could not be identified very accurately. For the $x=0$ sample we could not have the data below 130 K. But the trend of the data shows that α may reach a peak in this sample also at around the same temperature range as the other two samples. The hysteresis effects and magnitude of α in the temperature range $100<T<200$ K are time-dependent effects and they are expected to have a relation to the field sweep rate. Only the data for the field sweep rate of 0.01 T/sec are shown in Figs. 8 and 9. The data were taken at the field sweep rate of 0.005 T/sec, 0.01 T/sec, and 0.03 T/sec at selected temperatures. While at 4.2 K and above 200 K the differences between α for different field sweep rates are within 0.1%, in the temperature range 100–200 K α can differ by 5%. Generally α increases with increasing field sweep rate in 100–200 K range and hence it is very essential to remove the memory of the previously applied field by heating the sample to room temperature and cooling it to the prescibed temperature in zero field before starting any new measurement.

The above data also show that there are two distinct contributions to the MR (in the samples $x=0.07$ and $x=0.1$) and they show dominating effects at two temperature regions. One of them, associated with the cluster freezing or spin-glass-like transition, dominates at lower temperatures. The other, with very strong hysteresis effects, shows up at higher temperatures. Below we will try to identify the likely origins of these contributions in the light of the scenario we proposed above for the electronic transport.

In Fig. 10, we show a simple schematic of the hole transport in these materials (containing Co^{4+} in high-spin or low-spin states) as they hop from site to site. The other sites where the holes can go contain high-spin Co^{3+} ions. The relative population of the high-spin and low-spin trivalent cobalt ions will depend on temperature (as in the $x=0$ sample) as well as on the concentration of tetravalent Co ions created by Sr substitution. This is because, as has been argued in Ref. 18, a Co^{4+} (or Co^{IV}) stabilizes a high-spin Co^{3+} near it. As a result there is a relative clustering of high-spin Co^{3+} around a tetravalent Co ion and this stabilization is by lattice distortion and not by a thermal stabilization, unlike that in pure $LaCoO_3$. This allows us to distinguish between two types of high-spin Co^{3+}: (1) those created by thermal energy and whose population goes down because of the spin-state transition as the temperature is lowered below 100 K and (2) those created near a tetravalent Co ion by lattice stabilization which does not undergo a spin-state transition as the temperature is lowered. If we assume a strong Hund rule coupling which stabilizes the high-spin state, then for a carrier to go from one site to the other, the spin of the carrier has to be of correct orientation with respect to the total spin of the cation sitting on the site the carrier goes to. In fact it can be seen from Fig. 10 that the spins of the cations of the two sites have to be ferromagnetically aligned for maximum probability of hopping. For low-spin Co^{III} with $S=0$, this, however, is not an issue. The role of the magnetic field will therefore be to align the spins of the high-spin Co^{3+} and the Co^{IV} or Co^{4+} ions so that the hopping probability increases there by reducing the resistance and giving rise to the negative MR. On cooling below 100 K more high-spin Co^{3+} (which are not stabilized in a high-spin state around a tetravalent Co) undergo transition to zero moment carrying low-spin Co^{III} and as a result the effects of the spin alignments are of not much consequence to the hopping of the carriers and the effect of the magnetic field on transport is reduced. We think that this is happening in the $x=0$ sample. In this sample the hole (carriers) are thermally activated, and as a result there are very few Co^{4+} ions which are intentionally put in. Most of the Co^{3+} spins are therefore able to undergo a temperature-driven high-spin to low-spin transition. As a result the effect of the magnetic field on the transport is likely to diminish in the $x=0$ sample as T is lowered to near or below 100 K. At higher temperatures the parallel alignment of the Co^{3+} spins with that of the Co^{4+} or Co^{IV} spins will help transport and thus we find a negative MR. But the spins see a strong local random single-ion anisotropy which tends to hold them in a random orientation. Application of the field lowers the barriers and

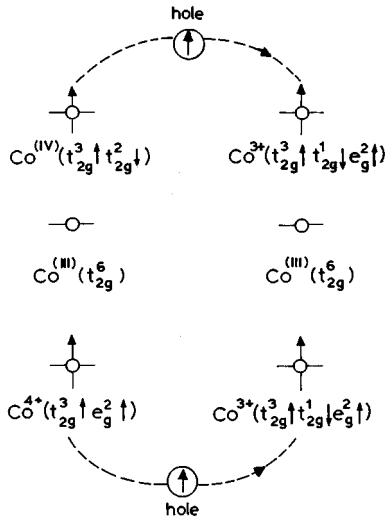

FIG. 10. A schematic diagram of hole transport in the cobaltates. The spin-conserving hole transfer from high-spin or low-spin tetravalent Co to high-spin trivalent Co gives rise to ferromagnetism and metallic behavior.

rotates the spins within certain length scales to parallel orientation. On removal of the field this orientation is retained and we see a strong hysteresis and resistivity nonclosure.

In the case of the $x=0.07$ sample and the $x=0.1$ sample there are two types of Co^{3+} ions. Near the tetravalent Co ions forming a ferromagnetically correlated region (or a cluster with a large spin) there will be stable Co^{3+} ions. In the space in between (the intercluster medium) there will be Co^{3+} ions which can undergo a transition to a low-spin state. At higher temperature the effects due to the intercluster medium will dominate, leading to a large hysteresis as in the $x=0$ sample. But as soon as the temperature goes below 100 K the effect of the magnetic field on the intercluster medium will go down. The effect of the magnetic field on the electronic transport within the cluster will then start to dominate. These clusters containing predominantly tetravalent Co and stable high-spin Co^{3+} have ferromagnetically correlated spins. The correlations become better at lower temperatures, leading to more MR at lower temperatures. However, when these clusters freeze in random orientations at the spin-glass-like transition T_g, the spins are also locked in random directions and this reduces the effect of the magnetic field on the spin orientation, leading to less MR.

To summarize, we find that the transport in the low-x insulating samples is controlled by the trivalent spins and their spin states. The hopping of the carrier from site to site is favored by a ferromagnetic spin alignment and the effect of the magnetic field is to create this alignment so that the resulting effect is a negative MR. The spin-state transition of the Co^{3+} ions affects the spins which are mainly unattached and do not belong to a ferromagnetic cluster consisting of tetravalent Co ions. As a result the magnetic field has effects on these ions as long as they are in the high-spin state. But for the trivalent Co ions which are stabilized by local distortion and attached to clusters, the spin-state transition does not take place and charge transport in these clusters is affected by the magnetic field even at low temperatures and the MR in this region is decided by the cluster dynamics.

VI. CONCLUSIONS

In this paper we have presented and tried to analyze the resistiviy and magnetoresistance data of a rather fascinating class of solids which actually show the spin-state transition of the transition metal. The important results of our experiment are the following.

(1) In the metallic compositions ($x \geqslant 0.2$) the MR is not substantial. It reaches a value of 4–8% at $T=T_c$. For the most metallic sample ($x=0.4$) there is a positive contribution near T_c in addition to the dominant negative MR. At low temperature MR becomes very small.

(2) For the composition close to the critical region $x \approx 0.2$, the cluster nature of the spin order shows up in MR. The magnitude of MR is still small ($<5\%$) but it shows peak in the temperature region where the cluster-freezing and/or spin-glass-like transition shows up.

(3) In the insulating samples ($x<0.2$) MR is large and negative and shows strong hysteresis effect. The origin of the hysteresis is explained as originating from the spin-state transition of Co ions.

(4) It also appears from our study that substantial negative MR can occur even when there are spin clusters instead of long-range ferrromagnetic order. The materials in this composition range are in the insulating state or in the critical region of the metal-insulator transition.

To our knowledge this is the first attempt to comprehensively study the MR in a solid showing a spin-state transition. There are a large number of issues related to the hysteresis effects observed in these materials which we did not discuss because we wanted to focus on the main issues in the paper. These effects are being looked into extensively and will be published elsewhere.

We also point out that the charge transport in this material has certain specialities in addition to the spin-state transition. In general materials showing VRH and ES type of hopping show positive MR at low temperatures due to orbital effects.[23] However, here we have hopping in the presence of spin interactions which give rise to large negative MR. But the interaction is not strong enough to modify the Coulomb gap occurring in the density of states near the Fermi level. When the material has more itinerant carriers and becomes metallic the screening will increase, leading to a short screening length, and the Coulomb gap formed by long-range interaction will vanish.

ACKNOWLEDGMENT

The authors thank the Department of Science and Technology, India, for financial support as a sponsored scheme.

[1] K. Chahara, T. Ohno, M. Kasai, and Y. Kozono, Appl. Phys. Lett. **63**, 1990 (1993).

[2] R. Von Helmolt, J. Wecker, B. Holzapfel, L. Schultz, and K. Samwer, Phys. Rev. Lett. **71**, 2331 (1993).

[3] M. McCormack, S. Jin, T. Tiefel, R. M. Fleming, J. M. Phillips, and R. Ramesh, Appl. Phys. Lett. **64**, 3045 (1995).

[4] H. L Ju, C. Kwon, Q. Li, R. L. Greene, and T. Venkatesan, Appl. Phys. Lett **65**, 2108 (1994).

[5] R. Mahesh, R. Mahendiran, A. K. Raychaudhuri, and C. N. R. Rao, J. Solid State Chem. **114**, 297 (1995).

[6] Y. Tokura, A. Urshibara, Y. Moritomo, T. Arima, G. Kido, and N. Furakawa, J. Phys. Soc. Jpn. **63**, 3931 (1994).

[7] R. Mahendiran, S. K. Tiwari, A. K. Raychaudhuri, T. V. Ramakrishnan, R. Mahesh, N. Rangavittal, and C. N. R. Rao, Phys. Rev. B **53**, 3348 (1996).

[8] Y. X. Jia, L. Lu, K. Khazeni, D. Yen, C. S. Lee, and A. Zettl, Solid State Commun. **94**, 917 (1995).

[9] H. Y. Hwang, S. W. Cheong, P. G. Radaelli, M. Marezio, and B. Batlogg, Phys. Rev. Lett. **75**, 914 (1995).

[10] P. Schiffer, A. P. Ramirez, W. Bao, and S. W. Cheong, Phys. Rev. Lett. **75**, 3396 (1996).

[11] J. F. Lawler and J. M. D. Coey, J. Magn. Magn. Mater. **140-144**, 2049 (1995).

[12] R. Mahendiran, A. K. Raychaudhuri, A. Chainani, and D. D. Sarma, J. Phys. Condens. Matter **7**, L561 (1995).

[13] S. Yamaguchi, H. Taniguchi, H. Takagi, T. Arima, and Y.

Tokura, J. Phys. Soc. Jpn. **54**, 1885 (1995).
[14] G. Briceno, H. Chang, X. Sun, P. G. Schultz, and X. D. Xiang, Science **270**, 273 (1995).
[15] G. H. Jonkar and J. H. VanSanten, Physica **19**, 120 (1953).
[16] V. G. Bhide, D. S. Rajoria, C. N. R. Rao, G. Rama Rao, and V. G. Jadhao, Phys. Rev. B **12**, 2832 (1975).
[17] P. Ganguly and C. N. R. Rao, in *Metallic and Non-metallic State of Matter*, edited by P. P. Edwards and C. N. R. Rao (Taylor & Francis, London, 1985).
[18] M. A. Senaris-Rodriguez and J. B. Goodenough, J. Solid State Chem. **118**, 323 (1995).
[19] M. Itoh, I. Natori, S. Kuboto, and K. Motoya, J. Phys. Soc. Jpn. **63**, 1486 (1994).
[20] P. Ganguly, P. S. Anil Kumar, P. N. Santhen, and I.S. Mulla, J. Phys. Condens. Matter **6**, 533 (1995).
[21] K. Asai, O. Yokokura, N. Nishimori, H. Chou, J. M. Tranquanda, G. Shrine, S. Higuchi, Y, Okajima, and K. Kohn, Phys. Rev. B **50**, 3025 (1994).
[22] H. Eisaki, T. Ido, K. Magoshi, M. Mochizuki, H. Yamatsu, and S. Uchida, Physica C **185–189**, 1295 (1991).
[23] B. I. Shlovskii and A. L. Efros, *Electronic Properties of Doped Semiconductors* (Springer-Verlag, Berlin, 1984).
[24] A. Chainani, M. Mathew, and D. D. Sarma, Phys. Rev. B **46**, 9976 (1992).
[25] A. K. Raychaudhuri, Adv. Phys. **44**, 21 (1996).
[26] R. Mahendiran, S. K. Tiwari, and A. K. Raychaudhuri (unpublished).
[27] S. C. Gausepohl, Mark Lee, K. Char, R. A. Rao, and C. B. Eom, Phys. Rev. B **52**, 3459 (1995).